JOURNAL OF SOLID STATE CHEMISTRY 34, 289–299 (1980)

Structure and Jahn–Teller Effect in Mixed Crystals $Rb_2Cr_{1-x}Mn_xCl_4$: A Single-Crystal Neutron Diffraction Study and Spectroscopic Results

G. MÜNNINGHOFF, W. TREUTMANN, AND E. HELLNER

Institut für Mineralogie der Universität, D 3550 Marburg, Federal Republic of Germany

G. HEGER

Kernforschungszentrum Karlsruhe, Institut für Angewandte Kernphysik, Postfach 3640, D 7500 Karlsruhe, Federal Republic of Germany

AND D. REINEN

Fachbereich Chemie der Universität, D 3550 Marburg, Federal Republic of Germany

Received July 26, 1979; in revised form November 2, 1979

The structures of single crystals $Rb_2Cr_{1-x}Mn_xCl_4$ ($0 \leq x \leq 1$) have been studied by neutron diffraction. A crystal of composition $x = 0.01$ shows a superstructure of the K_2NiF_4 type [space group *Bbcm*; $a = b = 7.262$ Å, $c = 15.733$ Å]. The structural refinement [$R = 0.043$] yields an antiferrodistortive order of tetragonally elongated octahedra (superimposed by a small orthorhombic component) with Cr–Cl bond lengths of 2.43 Å ($\parallel$[001]) and 2.40 Å, 2.74 Å ($\perp$[001]). Structural results for $x = 0.01/0.08/0.53/0.63/0.83/0.91/0.97$ in space group $I4/mmm$ [K_2NiF_4 type]—in particular the anomalous ms displacements of Cl(1) in the (001) plane—give evidence that the distortion of the (Mn, Cr)Cl_6 octahedra decreases with increasing x. AOM calculations based on experimental ligand field energies indicate that the individual $CrCl_6$ polyhedra are more strongly distorted than the (Jahn–Teller stable) $MnCl_6$ octahedra in mixed crystals with larger x values.

1. Introduction

Mixed crystals $Rb_2Cr_{1-x}Mn_xCl_4$ ($0 \leq x \leq 1$) represent an interesting example of a quasi two-dimensional magnetic system with ferromagnetic Rb_2CrCl_4 ($T_C = 53$ K) (*1*) and antiferromagnetic Rb_2MnCl_4 ($T_N = 57$ K) (*2*) as endmembers. The structures of the Cr and Mn compounds were first determined by Seifert *et al.* (*3, 4*) by means of X-ray powder diffraction. They both belong to the K_2NiF_4 type (Fig. 1). The NiF_6 octahedra are connected with each other by common corners in two dimensions and form infinite layers. These layers are held together by the K ions. As to Rb_2CrCl_4, X-ray and neutron powder data have been interpreted in terms of $CrCl_6$ octahedra, which are compressed in the direction of the tetragonal axis (*1, 3*). A distortion of this kind can be understood as the consequence of the Jahn–Teller effect, which lifts the or-

0022-4596/80/120289-11$02.00/0

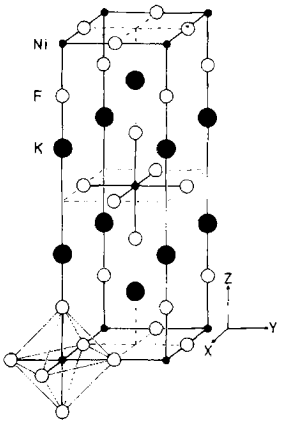

FIG. 1. The K_2NiF_4 structure.

bital degeneracy of the octahedral ^5E_g ground state. A compression of the $CrCl_6$ coordination is not in accord with the observed ferromagnetism of Rb_2CrCl_4, however. Only the assumption of an antiferrodistortive order of elongated octahedra (Fig. 5a), with alternately half-filled d_{z^2} and empty $d_{x^2-y^2}$ orbitals of Cr^{2+}, leads to the correct superexchange pattern and hence to a parallel spin–spin coupling in the basal planes (Fig. 2) (*5*). This argument is analogous to that of Khomski and Kugel (*6*) for the structurally related compound K_2CuF_4, which is a two-dimensional ferromagnet and contains the Jahn–Teller unstable d^9 cation Cu^{2+}. The antiferrodistortive model proposed by Khomski and Kugel for K_2CuF_4 has been suggested from EPR data also (Fig. 5a, (*7*)) and was verified by X-ray (*8*) and neutron diffraction (*9*). The unit cell of the K_2NiF_4 type has to be replaced by a larger superstructure cell. A similar antiferrodistortive order pattern may be suggested by Rb_2CrCl_4. NMR measurements by Le Dang Khoi and Veillet (*10*) and the observation of weak superstructure reflections by Day (*11*) which fit the proposed model give further support.

This paper reports about the increasing influence of the Jahn–Teller distortion in $Rb_2Cr_{1-x}Mn_xCl_4$ with increasing x. Also a detailed analysis of the superstructure on the Cr-rich side of the system ($x = 0.01$) is given. Finally, ligand field data are used to estimate the local deformation of the $CrCl_6$ octahedra in the Mn^{2+} rich mixed crystals.

2. Experimental Details

The mixed crystals were synthesized from stochiometric quantities of well-dried binary chlorides. Because the compounds are unstable to air and moisture they had always to be handled under dry and oxygen-free atmosphere. Single crystals were obtained by the vertical Bridgman–Stockberger method using lowering rates between 0.3 and 1.5 mm per hour. The temperature gradient was about 25 K/cm. Sample crystals with the shape of thin plates and volumes of about 30 mm^3 were used for the neutron diffraction experiment. To avoid decomposition they were sealed in thin-walled Al tubes, filled with He gas. This ensures good thermal contact during the low-temperature measurements which are presently performed to determine the magnetic structure. The neutron diffraction measurements were performed on the automatic four circle diffractometer P 110 at the reactor FR2/Kernforschungszentrum Karlsruhe. Using a wavelength of 0.92 Å complete data sets for seven compounds were taken at 298 K. Integral intensities up

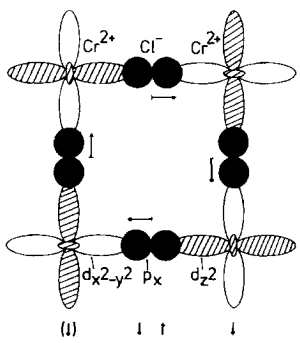

FIG. 2. Spin–spin coupling between d^4 cations in the (001) planes of Rb_2CrCl_4 [after D. Reinen (*5*); ↔, displacements of Cl^- ions].

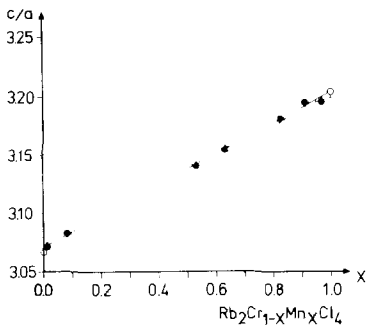

FIG. 3. The c/a ratio of the lattice constants in $Rb_2Cr_{1-x}Mn_xCl_4$ [○, values from literature (*1*, *2*)].

to sin $\Theta/\lambda \leq 0.78$ Å^{-1} were measured by the ω-scan technique. In this way a separation of the almost flat background is possible, even when using sample shieldings. The compositions of the mixed crystals have been determined by the structural refinement of the Cr/Mn ratio. Structure analyses in *I4/mmm* have been performed for the following stochiometries: x = 0.01/0.08/0.53/0.63/0.83/0.91/0.97. In Fig. 3 the ratio c/a of the lattice constants is plotted versus the manganese content. The dependence can be approximated by a straight line.

Neutron diffraction oscillation photographs[1] were taken on a crystal of composition $Rb_2Cr_{0.91}Mn_{0.09}Cl_4$ [$\lambda = 2.4$ Å, oscillation range 8°, time of exposure 22 hr] for the purpose of:

detecting superstructure reflections, which prove the existence of an *ordered* arrangement of distorted (Cr, Mn)Cl_6 octahedra,

distinguishing between different ordering possibilities between the (001) layers of the structure,

observing diffuse scattering caused by one-dimensional disorder of the layers.

In addition to the data sets for mixed crystals, which contain only reflections allowed in *I4/mmm*, a more detailed study was performed on a crystal of composition $Rb_2Cr_{0.99}Mn_{0.01}Cl_4$. Superstructure reflections compatible with the antiferrodistortive model of elongated $CrCl_6$ octahedra were measured under the same conditions as the basis structure reflections but with a three-times-longer measuring time.

3. Structural Refinement and Results

The structural model of elongated octahedra in antiferrodistortive order is not in accord with the symmetry of the space group *I4/mmm*. As we will show later the lower symmetry caused by the cooperative Jahn–Teller distortion leads to a subgroup of type *Cmca*. It is possible, however, to obtain reliable results with respect to the nature of the local Jahn–Teller distortions, even when the refinement is performed in *I4/mmm*.

Refinement in I4/mmm

Following the former work on Rb_2CrCl_4 (*3*) and Rb_2MnCl_4 (*4*) the atomic positions and positional parameters given in the subsequent tabulation have been taken as starting parameters for the refinement of $Rb_2Cr_{1-x}Mn_xCl_4$:

$(0, 0, 0; \frac{1}{2}, \frac{1}{2}, \frac{1}{2}) +$

(Cr, Mn)	in 2*a*, 4/*mmm*	0, 0, 0		
Rb	in 4*e*, 4*mm*	0, 0, z; 0, 0, $\bar{z}$	with $z = 0.35$	(1)
Cl(2)	in 4*e*, 4*mm*	0, 0, z; 0, 0, $\bar{z}$	with $z = 0.15$	
Cl(1)	in 4*c*, *mmm*	$\frac{1}{2}$, 0, 0; 0, $\frac{1}{2}$, 0		

[1] We have to thank Dr. Hohlwein (University of Tübingen) for providing the neutron diffraction camera P 111 (FR 2/Kernforschungszentrum Karlsruhe).

TABLE I

MIXED CRYSTALS $Rb_2Cr_{1-x}Mn_xCl_4$: UNIT CELL PARAMETERS (Å), ATOMIC POSITIONS, AND THERMAL TENSOR COMPONENTS (10^{-2} Å^2)

		x = 0.011(19)	x = 0.083(13)	x = 0.533(11)	x = 0.643(12)	x = 0.827(16)	x = 0.910(14)	x = 0.968(21)
	a	5.135(3)	5.127(3)	5.084(3)	5.083(3)	5.065(3)	5.056(3)	5.056(3)
	c	15.773(8)	15.806(8)	15.968(8)	16.035(8)	16.110(8)	16.152(8)	16.161(8)
	c/a	3.072(3)	3.083(3)	3.141(3)	3.155(3)	3.181(3)	3.195(3)	3.196(3)
(Cr, Mn)	$x = y = z$	0	0	0	0	0	0	0
	U	1.42(9)	1.42(6)	1.17(8)	1.25(9)	1.33(9)	1.48(6)	1.67(9)
Rb	$x = y$	0	0	0	0	0	0	0
	z	0.3602(1)	0.3598(1)	0.3587(1)	0.3583(1)	0.3581(1)	0.3578(1)	0.3575(1)
	$U_{11} = U_{22}$	3.53(16)	3.72(11)	3.33(11)	3.29(14)	3.27(15)	3.44(14)	3.29(20)
	U_{33}	1.84(9)	1.91(6)	2.29(6)	2.10(8)	1.85(8)	1.95(6)	1.72(10)
Cl(1)	$x = z$	0	0	0	0	0	0	0
	y	0.5	0.5	0.5	0.5	0.5	0.5	0.5
	U_{11}	2.09(8)	2.41(6)	2.60(6)	2.46(6)	2.32(8)	2.38(6)	2.33(9)
	U_{22}	5.40(13)	4.95(9)	2.22(5)	1.87(6)	1.34(6)	1.20(5)	1.01(8)
	U_{33}	3.57(9)	3.89(6)	3.46(5)	3.56(6)	3.29(6)	3.29(6)	3.25(9)
Cl(2)	$x = y$	0	0	0	0	0	0	0
	z	0.1542(1)	0.1543(1)	0.1553(1)	0.1557(2)	0.1562(1)	0.1565(1)	0.1564(1)
	$U_{11} = U_{22}$	3.88(14)	4.20(10)	3.95(10)	3.66(10)	3.39(11)	3.52(10)	3.32(14)
	U_{33}	1.30(6)	1.66(5)	1.74(4)	1.71(4)	1.44(5)	1.49(5)	1.44(6)
$R = \frac{\Sigma\|\|F_o\| - \|F_c\|\|}{\Sigma\|F_o\|}$		0.040	0.031	0.034	0.031	0.035	0.037	0.041

The z positional parameters and the anisotropic thermal factors of Rb^+ and Cl^-, as well as the Cr/Mn ratio and the isotropic temperature factor of (Cr, Mn), were used as free parameters. The results of the structural refinement are given in Table I. The reliability factor R ranges between 3 and 4%. The derived Me–Cl bond lengths are listed in Table II. Obviously the $MeCl_6$ octahedra in the mixed crystals with large x values are nearly undistorted. Also the thermal parameters of Cl(1) and Cl(2) are quite analogous in these cases. With decreasing x the Me–Cl distances perpendicular to the (001) planes become smaller and the in plane bond lengths slightly larger. This is in agreement with results of other authors (*1*, *3*) who report a tetragonally compressed $CrCl_6$ octahedron for Rb_2CrCl_4. The results in Table II are due to the fixed positional parameter of Cl(1) in $I4/mmm$, however, and don't represent the true (Cr, Mn)–Cl(1) bond lengths. The critical inspection of the ms displacements leads to the suggestion of a different local and cooperative distortion behavior, namely, an antiferrodistortive order of elongated octahedra (Fig. 5a).

The single-crystal data allowed us to include anisotropic temperature factors in the refinement. The dependence of the tensor components U_{11}, U_{22}, and U_{33}, describing

TABLE II

(CrMn)–Cl BOND LENGTHS (Å) IN $Rb_2Cr_{1-x}Mn_xCl_4$ (SPACE GROUP $I4/mmm$; STANDARD DEVIATION 0.002 Å)

	x						
	0.011	0.083	0.533	0.634	0.827	0.910	0.968
(Cr, Mn)–Cl(1) [4x]	2.567	2.563	2.542	2.541	2.532	2.528	2.528
(Cr, Mn)–Cl(2) [2x]	2.432	2.439	2.480	2.497	2.516	2.528	2.528

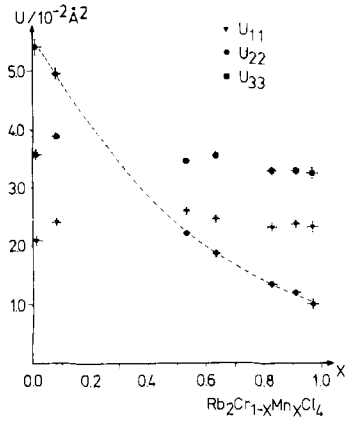

FIG. 4. The dependence of the ms displacements [U_{11}, U_{22}, U_{33}] of Cl(1) on the Cr^{2+} concentration in mixed crystals $Rb_2Cr_{1-x}Mn_xCl_4$ [U_{22}: component along (Cr, Mn)–Cl(1) bonds; refinement in *I4/mmm*].

the thermal ellipsoid of Cl(1), on the Cr^{2+} concentration (Table I) is illustrated in Fig. 4. U_{22}, the tensor component which extends along the Me–Cl bonds, behaves anomalously, increasing from 0.01 to 0.05 Å^2 between $x = 0.97$ and 0.01. A possible interpretation is that alternating long and short Me–Cl(1) bond distances in the [100] and [010] directions are covered by the increased U_{22} factors. Thus the space group *I4/mmm* can only give an averaged picture. A correct description of the structure has to include the superstructure reflections.

Model of the Superstructure

For the related compound K_2CuF_4 two stacking variants of the distorted perovskite-type layers were detected by crystal structure analysis. Ito and Akimitsu (*9*) describe the unit cell to be related to that of the K_2NiF_4 type by $a = 2^{1/2}a_0$ and $c = c_0$. Haegele and Babel (*8*) observed a doubling of the c-lattice constant in addition, with $a = 2^{1/2}a_0$ and $c = 2c_0$, a_0 and c_0 being the lattice constants of the K_2NiF_4 basic structure. Some disorder in the stacking of the layers was obvious from the diffuse intensity streaks which were observed in the [001] direction in this case also, however.

Our neutron scattering oscillation photographs which were taken around the a_0 and c_0 axes show additional weak reflections in agreement with the order proposed by Ito and Akimitsu. The observation of intensity along corresponding reciprocal lattice rods indicates that the ordering between the (001) planes is not complete. The structural model based on a unit cell with $a = 2^{1/2}\,a_0$ and $c = c_0$ allows the formation of two

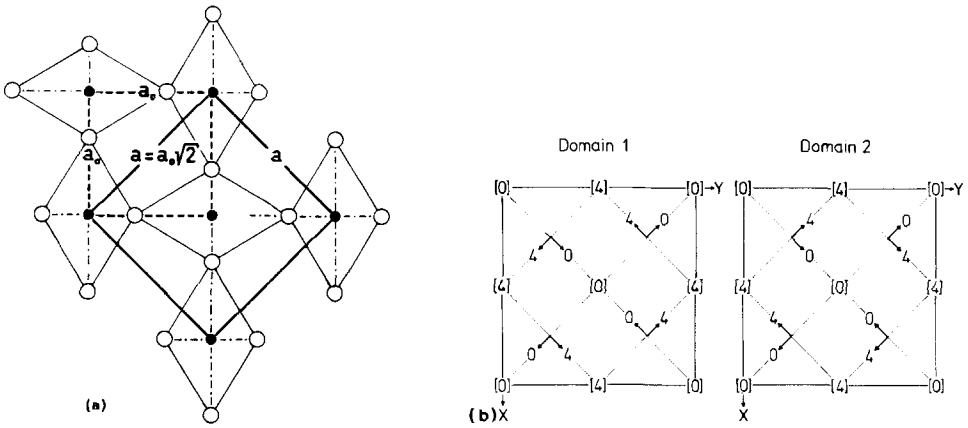

FIG. 5. The antiferrodistortive order of elongated $CrCl_6$ octahedra in the (001) planes of Rb_2CrCl_4. (a) Schematic drawing; (b) the two possibilities of domain formation in the antiferrodistortive model of Rb_2CrCl_4 [numbers in and without brackets: (Cr, Mn) and Cl(1) positions in units of 1/8c, respectively; the arrows indicate the directions of the long Cr–Cl(1) bond]. (b) is rotated by 45° with respect to (a).

domains, because the long Me–Cl bonds in the plane with $z = \frac{1}{2}$ have two possibilities of orientation with respect to those in the plane with $z = 0$ (Fig. 5b). Taking the same axes *a,b,c* for the two domains leads to the space groups *Bbcm* and *Acam* for domain 1 and domain 2, respectively. Both symbols correspond to the space group *Cmca* (No. 64) in the International Tables which is a subgroup of *I*4/*mmm* (Table III). The higher symmetry of the super group is indirectly conserved by domain formation. The orientation of the two domains to each other is due to the symmetry reduction.

The conditions for systematic absence of reflections for domain 1 and domain 2 and the resulting common systematic extinctions are the following:

	Bbcm	*Acam*	Resulting extinction
HKL	$H + L = 2n + 1$	$K + L = 2n + 1$	eeo, ooe
0*KL*	$K = 2n + 1$	$K = 2n + 1$	0o*L*, (0*K*o)
	$(L = 2n + 1)$	$(L = 2n + 1)$	
*H*0*L*	$H = 2n + 1$	$H = 2n + 1$	o0*L*, (*H*0o)
	$(L = 2n + 1)$	$(L = 2n + 1)$	(2)
*HK*0	$(H = 2n + 1)$	$(K = 2n + 1)$	—
*H*00	$(H = 2n + 1)$	$(H = 2n + 1)$	(o00)
0*K*0	$(K = 2n + 1)$	$(K = 2n + 1)$	(0o0)
00*L*	$(L = 2n + 1)$	$(L = 2n + 1)$	(00o)

e = even, o = odd.

The analysis of the diffractometer data of $Rb_2Cr_{0.99}Mn_{0.01}Cl_4$ showed full agreement with the "systematic extinctions" given above for the suggested superstructure model.

Data Treatment and Refinement in Bbcm

The superstructure cell is two times larger than the unit cell of the basic structure and contains four formular units of $Rb_2Cr_{0.99}Mn_{0.01}Cl_4$. In *Bbcm* the 4 (Cr, Mn), 8 Rb, and 16 Cl ions occupy the following atomic positions:

		(0, 0, 0; $\frac{1}{2}$, 0, $\frac{1}{2}$) +					
(Cr, Mn)	in 4*a*, $\frac{2}{m}$	0, 0, 0; 0, $\frac{1}{2}$, $\frac{1}{2}$					
Rb	in 8*d*,2	0, 0, *z*; 0, 0, $\bar{z}$; $\frac{1}{2}$,	$\frac{1}{2}$,	*z*;	$\frac{1}{2}$,	$\frac{1}{2}$,	$\bar{z}$ (3)
Cl(2)	in 8*d*,2	0, 0, *z*; 0, 0, $\bar{z}$; $\frac{1}{2}$,	$\frac{1}{2}$,	*z*;	$\frac{1}{2}$,	$\frac{1}{2}$,	$\bar{z}$
Cl(1)	in 8*f*,m	*x*, *y*, 0; $\bar{x}$, $\bar{y}$, 0; $\frac{1}{2} - x$,	$\frac{1}{2} + y$, 0;		$\frac{1}{2} + x$,	$\frac{1}{2} - y$, 0	

TABLE III

GROUP SUBGROUP RELATIONS[a] FOR $Rb_2Cr_{1-x}Mn_xCl_4$ (*16*)

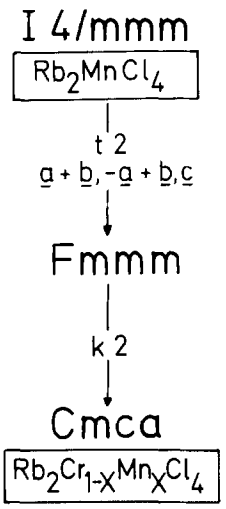

[a] The arrows represent transitions from a given space group into one of the maximal subgroups. t and k characterize transitions which don't affect the set of all translations and the crystal class, respectively. The index of symmetry reduction is also given.

The data set can be subdivided into four different kinds of reflections. Those with (eee) and (ooo) are compatible with the K_2NiF_4-type pseudocell. They are common to both domains, if H is equal to K. In the more general case $H \neq K$ a reflection (HKL) is (HKL) in domain 1 and (KHL) in domain 2. Only if x is equal to y for Cl(1) [tabulation (3)] (HKL) is symmetry equivalent to (KHL). Reflections (eoe) and (oeo) are superstructure reflections of domain 1, while superstructure reflections of domain 2 are of types (oee) and (eoo). From the intensity ratio of the corresponding superstructure reflections of the two domains the volume ratio v of domain 1 to domain 2 could be derived. For the 67 strongest pairs of superstructure reflections we obtained $v = 2.1(6)$. With this volume ratio the intensities of the superstructure reflections of domain 1 were scaled to the total volume of the investigated crystal.

In the first step of the refinement only the 335 inequivalent superstructure reflections of types (eoe) and (oeo) were considered. As scale factor the doubled value of that refined in *I4/mmm*—corresponding to the doubling of the K_2NiF_4 type unit cell—was used and not refined further more. The refinement of the positional and thermal parameters of Cl(1) yielded identical values for the positional parameters x and y within the standard deviations. The resulting R factor was 6.3%. Because x is equal to y, we could use the tetragonal average over the basic structure reflections ($I(HKL) = I(KHL)$ for (eee) and (ooo)). The atomic positions for Cl(1) from the first step of refinement were taken as starting parameters for the final refinement, in which all 600 inequivalent reflections were included. Table IV displays the refined parameters at an R factor of 4.3%. The tensor components U_{11} and U_{22} for Rb and Cl(2) were averaged, and the values for U_{12} were skipped.

TABLE IV

$Rb_2Cr_{0.989}Mn_{0.011}Cl_4$ ATOMIC PARAMETERS AND THERMAL TENSOR COMPONENTS (10^{-2} Å^2)
(SPACE GROUP *Bbcm*; $a = b = 7.262(4)$ Å, $c = 15.773(8)$ Å)

	x	y	z	U/U_{11}	U_{22}	U_{33}	U_{12}
(Cr, Mn)	0	0	0	1.48(5)			
Rb	0	0	0.3602(1)	3.46(9)	3.46(9)	1.94(6)	—
Cl(2)	0	0	0.1541(1)	3.89(6)	3.89(6)	1.27(4)	—
Cl(1)	0.26638(14)	0.26638(14)	0	2.01(4)	1.99(4)	3.69(5)	−0.03(4)

This is justified in view of the small deviation of the corresponding thermal ellipsoids from tetragonal behavior.

4. Discussion

Our main interest in the structural results of $Rb_2Cr_{0.99}Mn_{0.01}Cl_4$ concentrates on the geometry and the cooperative order of the (Cr, Mn)Cl_6 polyhedra. From Table IV the following bond distances were derived:

in plane (Cr, Mn)–Cl(1) bond lengths

$$\bar{A} + \Delta u(v) = A_u = 2.736(15)\ \text{Å}\ (2x);$$
$$\bar{A} + \Delta v(u) = A_v = 2.399(15)\ \text{Å}\ (2x),$$

out of plane (Cr, Mn)–Cl(2) bond length (4)

$$\bar{A} + \Delta z = A_z = 2.431(2)\ \text{Å}\ (2x),$$

average (Cr, Mn)–Cl bond length

$$[\Delta u + \Delta v + \Delta z = 0]$$
$$\bar{A} = 2.522(2)\ \text{Å}\ (6x).$$

This result shows unambigously an antiferrodistortive ordering of (essentially) tetragonally elongated (Cr, Mn)Cl_6 octahedra with the long axes in the (001) plane. The short (Cr, Mn)–Cl distances are slightly anisotropic, implying a small orthorhombic component of the tetragonal distortion. The radial and angular Jahn–Teller distortion parameters are $\rho = 0.37$ Å and $\varphi = 115°$, 245° [the two values refer to the two sublattices of elongated octahedra which constitute the antiferrodistortive order]. They are defined by (*12*)

$$\rho = 2^{1/2}\{(\Delta u)^2 + (\Delta v)^2 + (\Delta z)^2\}^{1/2};$$

$$tg\varphi = 3^{1/2}\,\frac{\Delta u - \Delta v}{2\Delta z - \Delta u - \Delta v} \quad (5)$$

[$\Delta i (i = u, v, z)$ as defined in tabulation (4)]. The atomic parameters resulting from the refinements in *Bbcm* and *I4/mmm* (Table IV and first column of Table I) show good agreement within the standard deviations for all atoms besides Cl(1). The anomalously increased tensor component U_{22} of Cl(1) in *I4/mmm* is obviously correlated with the deviation of Cl(1) from the ideal position $x = y = 0.25$ in *Bbcm*. Figure 6 shows an Ortep plot of the (Cr, Mn)–Cl_6 polyhedra in $Rb_2Cr_{0.99}Mn_{0.01}Cl_4$ after refinement in *I4/mmm* and in *Bbcm*, respectively. For comparison the (Cr, Mn)Cl_6 octahedron in a Mn-rich mixed crystal is also shown.

Under the assumption that the distortion of the octahedra is *tetragonal* the long (Cr, Mn)–Cl distances can be estimated for all investigated crystals. This distance is then the difference between the K_2NiF_4-type unit cell parameter a_0 in *I4/mmm* and the (Cr, Mn)–Cl(2) bond length in the z direction ($\bar{A} + \Delta z$ in tabulation (4); Table I). In Fig. 7 the experimental (Cr, Mn)–Cl(2) bond lengths are plotted together with the calculated long (Cr, Mn)–Cl(1) distances.

It is equally possible to estimate the underlying Jahn–Teller distortion from the thermal parameters, which characterize the (Cr, Mn)–Cl(1) bonds in the *I4/mmm* refinement (Table 1). In case of an anomalous thermal behavior in all octahedral directions the following equation is proposed by Ammeter *et al.* for calculation (*13*):

$$\rho \equiv 6^{1/2}\{\Delta U(M\text{–}L)_{\text{dyn.}} - \Delta U(M\text{–}L)_{\text{stat.}}\}^{1/2} \equiv 6^{1/2}\Delta U_{\text{JT}}^{1/2}. \quad (6)$$

The ΔU's are the differences between the ms displacements of the metal ion and the ligand atom along the M–L bond directions, in the dynamic (or averaged) and static

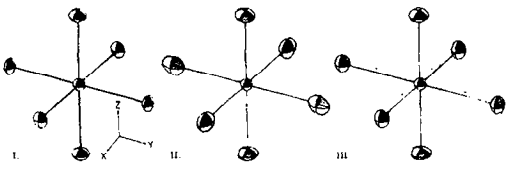

FIG. 6. Thermal ellipsoids of the (Cr, Mn)Cl_6 octahedra in $Rb_2Cr_{1-x}Mn_xCl_4$. (I) $x = 0.97$, refined in *I4/mmm*. (II, III) $x = 0.01$, refined in *I4/mmm* and *Bbcm*, respectively.

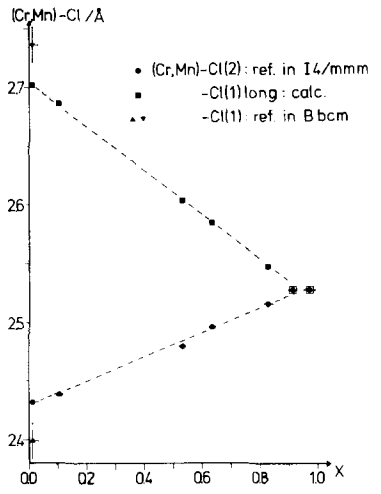

FIG. 7. Estimated (Cr, Mn)–Cl bond lengths in $Rb_2Cr_{1-x}Mn_xCl_4$ [assuming D_{4h} symmetry: $\Delta z = \Delta x = -\frac{1}{2}\Delta y$, tabulation (*4*)].

case, respectively. If the anomalous behavior of the thermal parameters is only two dimensional in nature a slightly modified equation may be used (12):

$$\rho \equiv 2^{1/2}\{2\Delta U_{\perp\perp}^{u,v} + (\Delta z)^2\}^{1/2}. \qquad (6a)$$

The application of the latter equation to the thermal parameters of the mixed crystal with $x = 0.01$ in space group *I4/mmm* (Table I) yields (Cr, Mn)–Cl(1) bond lengths (Table V), which are even more strongly anisotropic than those resulting from the refinement in *Bbcm* (tabulation (4)). For $x = 0.08$ the distortion of the (Cr–Mn)Cl_6 octahedra appears to be only slightly reduced compared to $x = 0.01$ ($\rho \simeq 0.41$ Å), while it is much smaller in case of $x = 0.53$. The bond lengths, obtained from the ms displacements, remain different down to $x \simeq 0.9$. In every case the calculation (Eq. (6a)) was based on the experimental (Cr, Mn)–Cl(2) bond length (Table II). The distortion parameters estimated by the assumption of D_{4h} symmetry (Fig. 7) and from the ms displacements seem to be smaller and larger than the experimental values, respectively.

Either from the thermal ellipsoids or from Fig. 7 metal–chlorine bond lengths are obtained, which are averaged values over $CrCl_6$ and $MnCl_6$ polyhedra. Possibly the former ones are more strongly distorted than the latter, however, particularly for higher x values. In order to get an idea about the *local* distortion of the individual $CrCl_6$ polyhedra we have measured the ligand field absorption of some mixed crystals [reflection spectra of ground single crystals] (Fig. 8).

The following consideration uses simple arguments of the "angular overlap model (AOM)" (*14*) and is based solely on the energy of the ligand field band, which corresponds to the transition within the Jahn–Teller split ^5E_g ground state. In D_{2h} symme-

TABLE V

BOND LENGTHS[a] AND JAHN–TELLER DISTORTION PARAMETERS (Å), FROM MS DISPLACEMENTS AND FROM LIGAND FIELD ENERGIES (10^3 cm^{-1}; 5 K VALUES; ASSIGNMENT IN D_{4h}), RESPECTIVELY

x	0.01[c]	0.53	0.83	0.91	Remarks
A_z, A_y	2.43	2.48	2.52	2.53	From Fig. 7[b]
A_u	2.70	2.60	2.55	2.53	$[D_{4h}]$
ρ	0.31	0.14	0.03	0	
A_v	2.36	2.43	2.47	2.48	From
A_u	2.77	2.65	2.59	2.58	thermal
ρ	0.44	0.23	0.12	0.09	parameters[d]
φ	111°	108°	98°	90°	$[D_{2h}]$
A_v	—	2.38	—	2.40	From
A_u	—	2.70	—	2.64	AOM
ρ	—	0.33	—	0.24	$[D_{2h}]^f$
φ	—	102°	—	90°	
$E[^5B_{1g} \rightarrow {}^5A_{1g}]$	7.5	6.6	—	$\simeq$4.8	Compare
$\rightarrow {}^5B_{2g}]$	$\simeq$10.0	$\simeq$9.8	—	—	Fig. 8
$\rightarrow {}^5E_g\ ]$	11.5_5	11.1_5	—	10.0	$[D_{4h}]$
Δ_0[e]	7.3	$\simeq$7.4	—	$\simeq$7.3	

[a] Defined in tabulation (4).

[b] Estimated from neutron diffraction data by assuming elongated D_{4h} symmetry.

[c] Experimental values from tabulation (4): $A_u = 2.73_5$ Å; $A_v = 2.40$ Å; $A_z = 2.43$ Å; $\rho = 0.37$ Å; $\varphi = 115°$ (245°).

[d] Based on $U(\text{Cr, Mn}) = 1.39 \times 10^{-2}$ Å^2 and $U(\text{Cl}(1))_{\text{stat.}} = 1.01 \times 10^{-2}$ Å^2 (compare Table I).

[e] Octahedral ligand field parameter $\Delta_0 = \frac{1}{3}[2E(^5E_g) + E(^5B_{2g})] - \frac{1}{2}E(^5A_{1g})$.

[f] Using the experimental A_z distances (Table II); because 5 K ligand field energies are used, the AOM distortion parameters actually refer to this temperature.

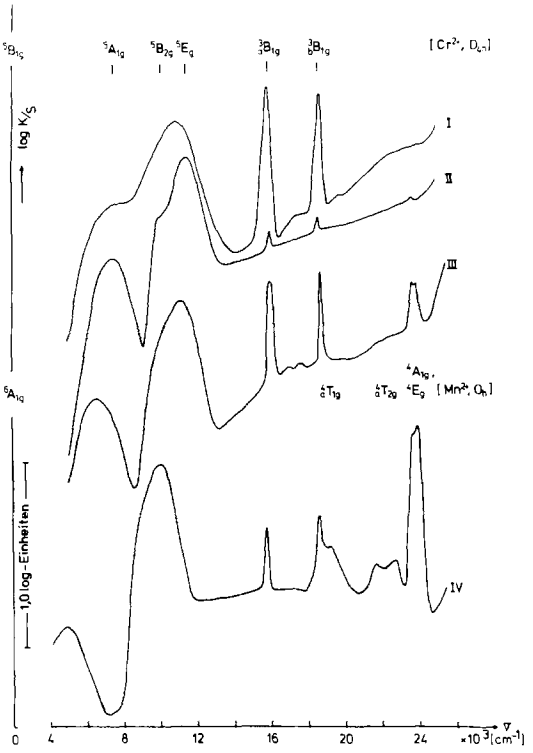

FIG. 8. Ligand field spectra of mixed crystals $Rb_2Cr_{1-x}Mn_xCl_4$: (I, II) $x = 0.01$, 298 and 5 K; (III) $x = 0.53$, 5 K; (IV) $x = 0.91$, 5 K. [(II) Assignment of $Cr^{II}Cl_6$ bands in D_{4h} symmetry (elongated): ${}^5E_g(O_h) \rightarrow {}^5B_{1g}$; ${}^5A_{1g}$; ${}^5T_{2g}(O_h) \rightarrow {}^5B_{2g}$, ${}^5E_g$; (IV) assignment of $Mn^{II}Cl_6$ bands in O_h symmetry.]

try the energy of this band can be expressed by

$$E({}^5_aA_g \rightarrow {}^5_bA_g) = 2\{e_\sigma^{u2} + e_\sigma^{v2} + e_\sigma^{z2} - e_\sigma^u e_\sigma^v - e_\sigma^v e_\sigma^z - e_\sigma^z e_\sigma^u\}^{1/2}. \quad (7)$$

If the local distortion of the $CrCl_6$ polyhedra is tetragonal, Eq. (7) simplifies to:

$$E({}^5B_{1g} \rightarrow {}^5A_{1g}) = 2(e_\sigma^{v,z} - e_\sigma^u). \quad (7a)$$

The energy parameters e_σ^i [i = u, v, and z, corresponding to Cr–Cl(1) and Cr–Cl(2) bond lengths, respectively] are defined by

$$e_\sigma^i = \frac{H_L}{H_M - H_L} S_\sigma^{i2} = K_\sigma \cdot S_\sigma^{i2}. \quad (8)$$

H_L and H_M are diagonal one-electron energies of the metal ion d orbitals and the ligand p orbitals, respectively. The S_σ^i's are tabulated overlap integrals (15). From the energy of the first band in the $Rb_2Cr_{0.99}Mn_{0.01}Cl_4$ spectrum (Table V) and the experimental Cr–Cl bond lengths (tabulation (4)) a K_σ parameter of $55._5 \times 10^4$ cm^{-1} results, using Eqs. (7) and (8). With this value of K_σ, the average Cr–Cl bond distance of 2.52 Å (tabulation (4)), and the experimental (Cr, Mn)–Cl(2) interatomic distances (Table II) we were able to estimate the Cr–Cl(1) bond lengths in all other mixed crystals (Table V), again utilizing Eqs. (8) and (7). The (Cr, Mn)–Cl(2) distances were considered to be almost equal for the individual $CrCl_6$ and $MnCl_6$ polyhedra, because the temperature factors don't indicate anomalous behavior (Table I).

The Cr–Cl(1) bond lengths estimated from AOM energies deviate appreciably from those, which are obtained from the ms displacements or the simple procedure of Fig. 7. Even if one regards the AOM calculation as a rough estimate only, one may conclude that the Jahn–Teller deformations of the individual $CrCl_6$ octahedra are larger than those distortions which characterize the $MnCl_6$ polyhedra, particularly at lower Cr^{2+} concentrations. The distortion may be static or dynamic, however (see below). The very distinct orthorhombic distortion component can be substantially reduced by assuming that the Cr–Cl(2) bonds are slightly shorter than the experimental (Cr, Mn)–Cl(2) distances.

It is remarkable that the (Cr, Mn)Cl_6 polyhedra in the mixed crystals with $x > 0.9$ are regular (Table II). This is not required by the symmetry of the K_2NiF_4 space group. Usually the octahedra are slightly compressed along the tetragonal c axis in compounds with the K_2NiF_4 structure. It is further interesting that the octahedra, which are regular at 298 K, become tetragonally elongated when lowering the temperature. In the mixed crystal with $x =$

0.97 for example the isotropic (Mn, Cr)–Cl bond lengths of 2.528(2) Å (Table II) change to 2.512(2) Å [in plane] and 2.526(2) Å [out of plane] at 20 K.

Finally we raise the question, whether the Jahn–Teller distortion of the $CrCl_6$ octahedra in the mixed crystals $Rb_2Cr_{1-x}Mn_xCl_4$ is static or dynamic at 298 K. We may suggest that a static Jahn–Teller distortion is already present, if the (Cr, Mn)–Cl(2) bond length is significantly different from the (Cr, Mn)–Cl(1) distances. This argument bases on the result of *regular* $MnCl_6$ "host lattice sites." Definite evidence for a static deformation is only the presence of superstructure reflections, however. Otherwise the Jahn–Teller distortion may be dynamic in the (001) planes. At very large x values ($x \gtrsim 0.9$) the deformation of the $CrCl_6$ octahedra is likely to be 3-dimensionally dynamic at 298 K. Neutron diffraction measurements on Cr-rich mixed crystals in dependence on temperature are in progress, in order to characterize possible static to dynamic transitions.

In a very recent paper, published after the submittal of this contribution, preliminary results of a low-temperature neutron diffraction study of the end member of the mixed crystal series, Rb_2CrCl_4 are reported (*17*). The 77 K Cr–Cl bond lengths A_u = 2.700(1) Å, A_v = 2.379(1) Å, and A_z = 2.357(24) Å are in reasonable agreement with our 298 K data for the mixed crystal with x = 0.01 (tabulation (4)). Taking the slightly smaller average bond distance at 77 K into account, only a significant divergence in the out-of-plane direction remains, which is probably induced by the large A_z standard deviation in (*17*). It should also be mentioned that the structure analysis by Day *et al.* (*17*) is based on about 100 inequivalent reflections, while a complete data set within the range $\sin\Theta/\lambda \leq 0.78$ Å^{-1} (600 inequivalent reflections) was used in this study.

Acknowledgments

We gratefully acknowledge financial support by the "Bundesministerium für Forschung und Technologie (BMFT)." Further we have to thank Mr. N. Lessmann for technical assistance in growing the single crystals and Mr. M. Weber for preparative work and taking the 5 K ligand field spectra.

References

1. M. J. Fair, A. K. Gregson, P. Day, and M. T. Hutchings, *Physica (The Hague)* **86-88B**, 657 (1977).
2. A. Epstein, E. Gurewitz, J. Makowsky, and H. Shaked, *Phys. Rev. B* **2**, 3703 (1970).
3. H. J. Seifert and K. Klatyk, *Z. Anorg. Allg. Chem.* **334**, 113 (1964).
4. H. J. Seifert and F. W. Koknat, *Z. Anorg. Allg. Chem.* **341**, 269 (1965).
5. D. Reinen, P. Koehler, and W. Massa, *in* "Proceedings, 19th Int. Conf. Coord. Chem. Prague, 1978," Vol. I, p. 153.
6. D. J. Khomskii and K. J. Kugel, *Solid State Commun.* **13**, 763 (1973).
7. C. Friebel and D. Reinen, *Z. Anorg. Allg. Chem.* **407**, 193 (1974).
8. R. Haegele and D. Babel, *Z. Anorg. Allg. Chem.* **409**, 11 (1974).
9. Y. Ito and J. Akimitsu, *J. Phys. Soc. Japan* **40**, 1333 (1976).
10. K. Le Dang, P. Veillet, and P. J. Walker, *J. Phys. C* **10**, 4593 (1977).
11. M. J. Fair, M. T. Hutchings, P. Day, R. Gosh, and P. J. Walker, *J. Phys. C* **11**, L813 (1978).
12. D. Reinen and C. Friebel, "Structure Bonding," Vol. 37, p. 7, Springer-Verlag, Berlin/New York (1979).
13. J. H. Ammeter, H. B. Buergi, E. Gamp, V. Meyer-Sandrin, and W. P. Jensen, *Inorg. Chem.* **18**, 733 (1979).
14. e.g. C. E. Schaeffer and C. K. Jørgensen, *Mol. Phys.* **9**, 401 (1965).
15. S. Kremer, to be published.
16. G. Heger, D. Mullen, and K. Knorr, *Phys. Status Solidi (a)* **35**, 627 (1976).
17. P. Day, M. T. Hutchings, E. Janke, and P. J. Walker, *J. Chem. Soc. Chem. Commun.*, 711 (1979).